Rev.Adv.Mater.Sci. 7 (2004) 75-82

PARTIAL AND SPLIT DISLOCATIONS IN DEFORMED NANOCRYSTALLINE METALS

S.V. Bobylev and I.A. Ovid'ko

Institute of Problems of Mechanical Engineering, Russian Academy of Sciences, Bolshoj 61, Vas. Ostrov, St. Petersburg 199178, Russia

Received: July 16, 2004

Abstract. A theoretical model is suggested that describes partial and split dislocation configurations in deformed nanocrystalline metals. Ranges of parameters (grain size, applied stress, etc.) are calculated in which these dislocation configurations are energetically favorable. The model accounts for experimental data (Liao *et al*, Appl. Phys. Lett. **84** (2004) 3564) on observation of anomalously wide stacking faults that join partial dislocations in nanocrystalline aluminium.

1. INTRODUCTION

Nanocrystalline materials exhibit unique mechanical properties that represent the subject of rapidly growing fundamental and applied research efforts; see, e.g., [1–5]. The outstanding mechanical behavior of nanocrystalline materials is due to their specific nanoscale structure causing the very important role of grain boundaries in deformation and failure processes. In particular, high-density ensembles of grain boundaries are treated to intensively conduct such deformation modes as grain boundary sliding [6–10], Coble creep [10–13] and rotational deformation [14–18] in nanocrystalline materials with finest grains. In addition, as shown in recent experiments [19–23], grain boundaries serve as effective sources of partial dislocations (Fig. 1a) that carry twin deformation in nanocrystalline materials. These partial dislocations often form split dislocation configurations each representing a pair of partials joint by a stacking fault (Fig. 1b). The two specific behavioral features of partial and split dislocations in nanocrystalline materials have been experimentally detected. First, emission of partial and split dislocation configurations from grain boundaries is enhanced with decreasing grain size [19–23]. Second, stacking faults that join partial dislocations emitted from grain boundaries in nanocrystalline Al are characterized by width values being larger by several times that those in coarse-grained Al samples [23]. The former experimental fact has been recently analysed in the framework of the model describing structural transformations of dislocated grain boundaries in deformed nanocrystalline materials [24]. The second experimental fact – the formation of anomalously wide stacking faults in deformed nanocrystalline Al – has been discussed in terms of the first approximation model [23] which, however, does not take into account structural transformations of grain boundaries due to emission of partial dislocations. At the same time, the role of such structural transformations (associated with changes in the nanoscale stress distribution in vicinities of grain boundaries) can not be ignored in a theoretical description of partial dislocations, since characteristic length scales of the

Corresponding author: I.A. Ovid'ko, e-mail: ovidko@def.ipme.ru

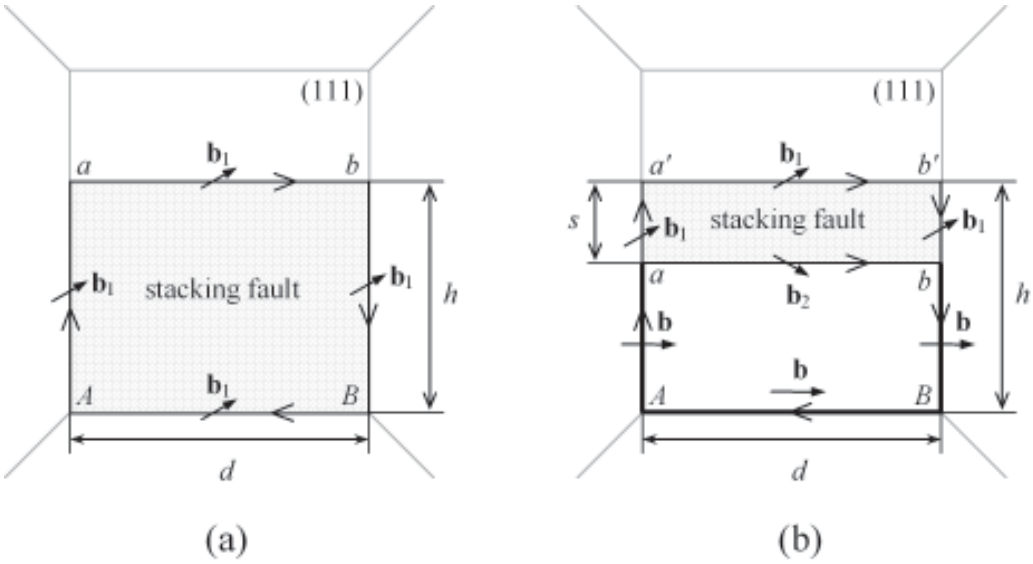

Fig. 1. Partial and split dislocations emitted by grain boundary *AB*. (a) Partial Shockley dislocation *ab* is emitted by grain boundary. As a result, rectangular dislocation loop *abBA* is formed which bounds stacking fault (shaded region). (b) Two partial Shockley dislocations *ab* and *a'b'* are emitted from grain boundary *AB*. As a result, the rectangular stacking fault *abb'a'* is formed which bounds rectangular dislocation loop *abb'a'* with the edge dislocation segments *aa'* and *bb'*. Also, screw dislocation segment *AB* characterized by Burgers vector $\boldsymbol{b} = \boldsymbol{b}_1 + \boldsymbol{b}_2$ is formed at grain boundary.

dislocation configurations in nanocrystalline materials are in the nanometer range. The main aim of this paper is to suggest a theoretical model describing partial and split dislocation configurations in deformed nanocrystalline metals and taking into account structural transformations of grain boundaries emitting such dislocation configurations.

2. PARTIAL AND SPLIT DISLOCATIONS IN NANOCRYSTALLINE METAL. MODEL

In the framework of our our model, we consider a crystalline grain with square slip plane (111) and its adjacent boundary *AB* (Fig. 1). The grain boundary *AB* emits the partial Shockley dislocation *ab* with Burgers vector $\boldsymbol{b}_1 = a/6\,[2\bar{1}\bar{1}]$ as shown in Fig. 1a. In these circumstances, in accordance with the Burgers vector conservation law, the rectangular dislocation loop configuration *AabB* is formed which bounds the rectangular stacking fault *AabB* (Fig. 1a). The stacking fault is characterized by the energy density γ (per unit area of the stacking fault plane) which specifies the hampering force for both emission and movement of the partial dislocation *ab*. The emission of partial dislocations from grain boundaries in deformed nanocrystalline materials has been theoretically analysed by Bobylev *et al* [24]. The model [24] describes the emission of sole partial dislocations (Fig. 1a) and its sensitivity to the initial dislocation structure of grain boundaries, but does not consider the experimentally observed [23] split dislocations (Fig. 1b). Since the main aim of this paper is to explain the experimentally observed [23] formation of anomalously wide stacking faults in deformed nanocrystalline Al, here we focus our consideration on the stacking fault width as a characteristic of split dislocations emitted from grain boundaries. In these circumstances, details of the initial dislocated structure of grain boundaries are not essential for our analysis. We consider the only dislocation segments *AB* resulted from emission of partial and split dislocations (Fig. 1), whereas the effects of the initial dislocated structure (existing before the emission events) of the grain boundary are neglected.

Now let us turn to the situation where the second Shockley dislocation *a'b'* with Burgers vector $\boldsymbol{b}_2 = a/6\,[1\bar{2}1]$ is emitted from the grain boundary as shown in Fig. 1b. In accordance with the Burgers vector conservation law, the Shockley dislocation

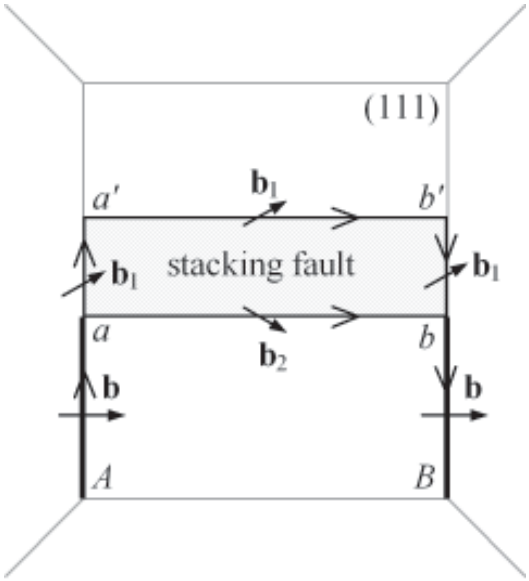

Fig. 2. Dislocation model [23] of the wide stacking fault formation. Two Shockley dislocations, *ab* and *a'b'*, are consequently emitted by grain boundary *AB* which is free from dislocations after the emission events. Dislocation segments *Aa* and *Bb* join the Shockley dislocations and grain boundary junctions *A* and *B*.

a'b' is joint by the perfect edge dislocation segments *Aa'* and *Bb'* with the grain boundary junctions *A* and *B*. Also, the rectangular loop *abb'a'* with the Shockley dislocation segments is formed which bounds the rectangular stacking fault *abb'a'* (Fig. 1b). In paper [23], it has been assumed that the grain boundary *AB* is free from dislocations, but is connected by the edge dislocation segments *Aa'* and *Bb'* with the second Shockley dislocation (Fig. 2). This assumption ignores structural transformations of the grain boundary *AB* after the dislocation emission events and does not consider the Burgers vector conservation law at the boundary junctions *A* and *B*. In the framework of our model, we suppose that, in accordance with the Burgers vector conservation law, the emission of the Shockley dislocations *ab* and *a'b'* from the grain boundary *AB* is accompanied by the formation of the screw dislocation with Burgers vector $\boldsymbol{b}=a/2\,[1\bar{1}0]$ at this boundary. (Burgers vector **b** is equal to the sum Burgers vector $\boldsymbol{b}_1+\boldsymbol{b}_2$ of the two Shockley dislocations *ab* and *a'b'*, whereas directions of screw and Shockley dislocation line segments are opposite.) In these circumstances, the elastic interaction between the Shockley dislocations and the residual screw dislocation *AB* at the grain boundary comes into play. This interaction has been ignored in the first approximation model [23], but can essentially contribute to the energy characteristics of the dislocation configurations under consideration (Fig. 1).

In the next section, we will estimate and compare the energy characteristics of the two dislocation configurations shown in Figs. 1a and b, that is, the configurations with respectively one and two Shockley dislocations emitted from the grain boundary *AB*. This will allow us to reveal the ranges of parameters of the system, at which the dislocation configurations (Fig. 1) are energetically favorable.

3. ENERGY CHARACTERISTICS OF PARTIAL AND SPLIT DISLOCATIONS EMITTED FROM GRAIN BOUNDARY

First, let us consider the energy of the configuration with one Shockley dislocation emitted from the grain boundary *AB* (Fig. 1a). This energy E_1 consists of seven terms:

$$E_1 = E_1^{AB-ab} + E_1^{ab} + E_1^{AB} + E_1^{Aa} + E_1^{Bb} + E_{c1} + E_{\gamma 1}. \quad (1)$$

Here E_1^{AB-ab} is the energy that characterizes the elastic interaction between the dislocation segments *AB* and *ab*; E_1^{ab}, $E_1^{a'b'}$, E_1^{Aa} and E_1^{Bb} are the proper energies of the dislocation segments *ab*, *a'b'*, *Aa* and *Bb*, respectively; E_{c1} is the sum energy of the dislocation cores; $E_{\gamma 1}$ is the total energy of the stacking fault. The grain size *d* in nanocrystalline materials commonly plays the role of the characteristic length scale of structural inhomogeneities and stress field distribution. In these circumstances, in estimates of the dislocation energy terms in formula (1), the grain size *d* is chosen as the screening length of the dislocation stress fields. With this assumption, the energies that characterize the interaction between perpendicular dislocation segments and that between parallel dislocation segments *Aa* and *Bb* distant by *d* from each other are low compared to the energies figuring on the right hand side of the formula (1) and thereby are not taken into our consideration.

Following the theory of dislocations in solids [25], the energies figuring in formula (1) are written as:

$$E_1^{AB-ab} = -\frac{Gb_1^2 d(1-\nu\sin^2\alpha)}{2\pi(1-\nu)}\ln\frac{R}{h},$$

$$E_1^{ab} = E_1^{AB} = \frac{Gb_1^2 d(1-\nu\sin^2\alpha)}{4\pi(1-\nu)}\ln\frac{R}{r_0},$$

$$E_1^{Aa} = E_1^{Bb} = \frac{Gb_1^2 h(1-\nu\cos^2\alpha)}{4\pi(1-\nu)}\ln\frac{R}{r_0},$$

$$E_{\gamma 1} = \gamma dh, \qquad (2)$$

$$E_{c1} = \frac{Gb_1^2 d(1-\nu\sin^2\alpha)}{4\pi(1-\nu)} + \frac{Gb_1^2 h(1-\nu\cos^2\alpha)}{4\pi(1-\nu)}.$$

Here G denotes the shear modulus, ν the Poisson ratio, h the distance between the partial Shockley dislocation ab and the grain boundary AB (see Fig. 1a), $\alpha = 60°$ the angle between Burgers vector and line core of the partial dislocation, R the screening length of the dislocation stress fields, r_0 the dislocation core radius (assumed to be the same for all the dislocations under consideration), and γ the specific energy of the stacking fault. For $R=d$, $r_0=b$, $b = a/\sqrt{2}$ and $b_1 = a/\sqrt{6}$, substitution of formulas (2) into the expression (1) yields the following formula for the energy E_1:

$$E_1 = \frac{Ga^2}{48\pi(1-\nu)}\left[d(3\nu-4)\ln\frac{d}{h} + (d(4-3\nu)+h(4-\nu))\left(\ln\frac{\sqrt{2}d}{a}+1\right)\right] + \gamma dh. \qquad (3)$$

The energy E_2 of the dislocation configuration with two partial dislocations emitted from the grain boundary AB (Fig. 1b) has twelve terms:

$$E_2 = E_2^{ab-a'b'} + E_2^{AB-ab} + E_2^{AB-a'b'} + E_2^{ab} + E_2^{a'b'} + E_2^{Aa'} + E_2^{Bb'} + E_2^{aa'} + E_2^{bb'} + E_2^{AB} + E_{c2} + E_{\gamma 2}. \qquad (4)$$

Here $E_2^{ab-a'b'}$ denotes the energy that characterizes the elastic interaction between the partial dislocation segments ab and $a'b'$; E_2^{AB-ab} and $E_2^{AB-a'b'}$ are the energies that characterize the interaction between the screw dislocation segment AB and respectively the partial dislocation segments ab and $a'b'$; E_2^{ab}, $E_2^{a'b'}$, $E_2^{Aa'}$, $E_2^{Bb'}$, $E_2^{aa'}$, $E_2^{bb'}$ and E_2^{AB} are the proper energies of the dislocation segments ab, $a'b'$, Aa', Bb', aa', bb' and AB, respectively; E_{c2} is the sum energy of the dislocation cores; $E_{\gamma 2}$ is the total energy of the stacking fault. (In deriving formula (4), we have used the same simplifying assumptions, as with formula (1).)

Following the standard dislocation theory [25], the energies figuring on the right hand side of formula (4) are given as:

$$E_2^{ab-a'b'} = -\frac{Gb_1^2(\cos 2\alpha + \nu\sin^2\alpha)}{2\pi(1-\nu)}\ln\frac{R}{s},$$

$$E_2^{AB-ab} = -\frac{Gbb_1 d\sin\alpha}{2\pi}\ln\frac{R}{h},$$

$$E_2^{AB-a'b'} = -\frac{Gbb_1 d\sin\alpha}{2\pi}\ln\frac{R}{h-s},$$

$$E_2^{ab} = E_2^{a'b'} = \frac{Gb_1^2 d(1-\nu\sin^2\alpha)}{4\pi(1-\nu)}\ln\frac{R}{r_0},$$

$$E_2^{Aa'} = E_2^{Bb'} = \frac{Gb^2(h-s)}{4\pi(1-\nu)}\ln\frac{R}{r_0},$$

$$E_2^{aa'} = E_2^{bb'} = \frac{Gb_1^2 s(1-\nu\sin^2\alpha)}{4\pi(1-\nu)}\ln\frac{R}{r_0},$$

$$E_2^{AB} = \frac{Gb^2 d}{4\pi}\ln\frac{R}{r_0},$$

$$E_{\gamma 2} = \gamma ds, \qquad (5)$$

$$E_{c2} = \frac{Gb_1^2 d(1-\nu\cos^2\alpha)}{2\pi(1-\nu)} + \frac{Gb_1^2 s(1-\nu\sin^2\alpha)}{2\pi(1-\nu)} + \frac{Gb^2(h-s)}{2\pi(1-\nu)} + \frac{Gb^2}{4\pi}.$$

Here s is the stacking fault width. For the same values of characteristic parameters as with the dislocation configuration shown in Fig. 1a, we have the following expression for the energy E_2:

$$E_2 = \frac{Ga^2}{48\pi(1-\nu)}\left[d(2-3\nu)\ln\frac{d}{s} - 6d(1-\nu)\ln\frac{d^2}{h(h-s)} + (d(4-3\nu)+12(h-s)+s(4-\nu)+12(1-\nu)d)\left(\ln\frac{\sqrt{2}d}{a}+1\right)\right] + \gamma ds. \qquad (6)$$

Now let us take into consideration the action of the external stress on the dislocations. Let the edge components of the partial dislocations be under the

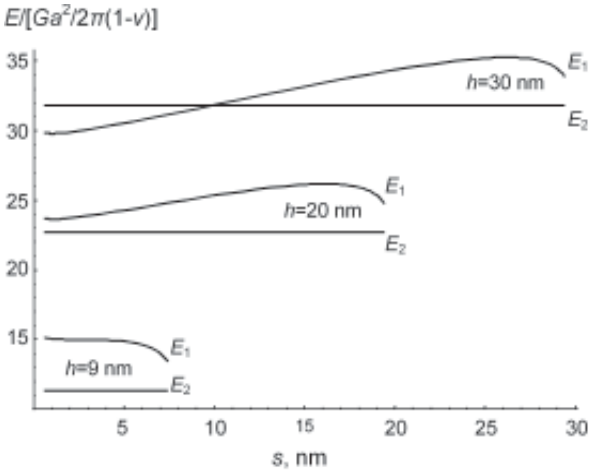

Fig. 3. Dependences of the energies E_1 and E_2 of the dislocation configurations shown in respectively Fig. 1a and b on stacking fault width *s* (distance between Shockley dislocations *ab* and *a'b'*) at various values of parameter *h*.

shear stress t action which causes the driving force for expansion of the stacking fault. In the situations with one and two partial dislocations (see Figs. 1a and b, respectively), the driving force is given as $f_1=2\tau b_\perp=\tau a/\sqrt{6}$ and $f_2=\tau b_\perp=\tau a/2\sqrt{6}$, respectively, where $b_\perp=b_1\sin30°$ is the edge component of Burgers vector $\boldsymbol{b}_1$. In these circumstances, the external stress action is described by use of the following effective values of the stacking fault energy densities γ_1 and γ_2 corresponding to the configurations with one and two partial dislocations, respectively:

$$\gamma_1=\gamma-\frac{\tau a}{2\sqrt{6}},$$
$$\gamma_2=\gamma-\frac{\tau a}{\sqrt{6}}. \qquad (7)$$

With γ replaced by γ_1 and γ_2 in the expressions (3) and (6), respectively, one finds the dependences of the characteristic energies E_1 and E_2 on the shear stress τ.

Comparison of values of the energies E_1 and E_2 and their dependences on parameters of the system allows us to reveal the energetically favorable configuration – either the configuration with one Shockley dislocation *ab* (Fig. 1a) or the configuration with two Shockley dislocations *ab* and *a'b'* (Fig. 1b) – at given values of the parameters. In doing so, in our calculations, we have used the following characteristic values of parameters for Al: *G*=35 GPa, ν=0.345, *a*=0.404 nm, γ=0.122 J/m^2 [23]. For illustration, the dependences of E_1 and E_2 on the stacking fault width *s* are shown in Fig. 3, for the grain size *d*=50 nm, τ=0 and various values of *h*. E_1 is constant at a constant value of *h* = *s*, in which case $E_1(s)$ represents a horizontal line at given *h*. For *h*=30 nm, we have $E_2(s)<E_1$ at some values of *s*, and the dependence $E_2(s)$ has a minimum that corresponds to the equilibrium width s_0 of the stacking fault. That is, for given values of *d* and *h*, the configuration with two Shockley dislocations (distant by s_0 from each other) is energetically favorable. However, with decreasing *h* at the same value of the grain size *d*, curve $E_2(s)$ can lie above the horizontal line $E=E_1$, for any value of *s*. This situation is illustrated by curves $E_2(s)$ corresponding to *h*=9 and 20 nm in Fig. 3.

Notice that the dependence $E_2(s)$ at low *h* monotonously decrease with rising *s*, and $E_2(s)>E_1$; see lower curves in Fig. 3. If both monotonous and non-monotonous (with a minimum) curves $E_2(s)$ lie above the horizontal line $E=E_1$, the emission of two Shockley dislocations from the grain boundary *AB* (Fig. 1b) is not favorable; the configuration with one Shockley dislocation (Fig. 1a) is preferred.

Our calculations are indicative of the following tendencies. The formation of pairs of Shockley dislocations (Fig. 1b) is energetically unfavorable in finest grains. More precisely, if $d<d_c$=36 nm, $E_1<E_2$ at any values of *h* and *s*, that is, the configuration with one partial dislocation is energetically favorable. The critical grain size d_c grows with rising the shear stress τ (see Fig. 4a).

For low values of *h,* the configuration with two Shockley dislocations is unfavorable. When $h\geq h_c$, this configuration (Fig. 1b) becomes energetically preferred ($E_2<E_1$ in some range of *s*). The critical value h_c depends on the grain size *d*; it is illustrated by curves $h_c(d)$ in Fig. 4b, for various values of τ.

4. STACKING FAULT WIDTH IN NANOCRYSTALLINE METALS

Let us use results of our calculation of the energy E_2 (see previous section) in consideration of the stacking fault width s_0 that characterizes the split dislocation configuration (Fig. 1b). To do so, let us analyze the dependence of the stacking fault width s_0 on *d* and compare it with that in coarse-grained polycrystals and results of paper [23]. In contrast to the model [23], in our model, s_0 depends on both *d* and *h* (because of the elastic interaction between

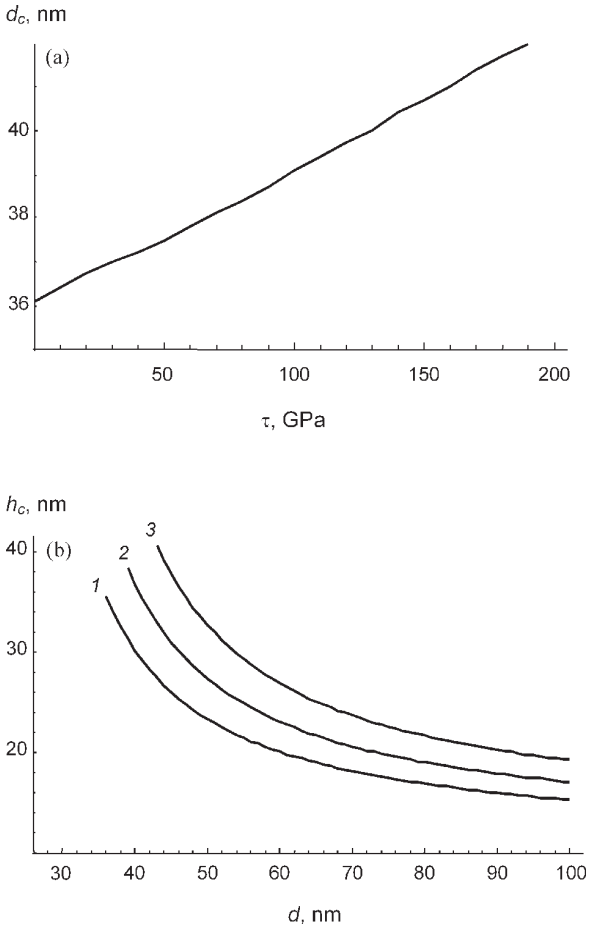

Fig. 4. (a) Dependence of critical grain size d_c on the shear stress τ. (b) Dependence of critical value h_c (see text) on the grain size d at τ=0 (curve *1*), τ=100 MPa (curve *2*) and τ=200 Mpa (curve *3*).

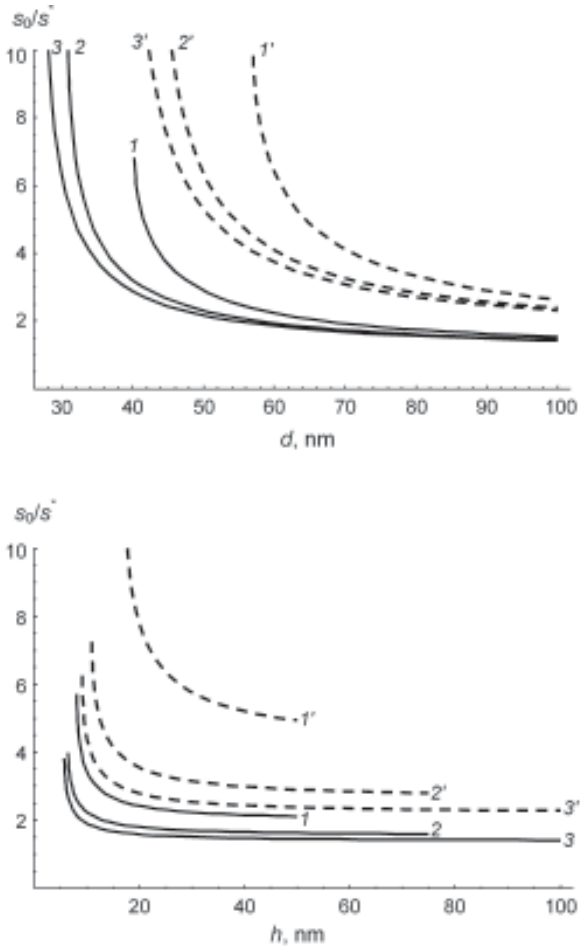

Fig. 5. Dependences of ratio s_0/s^* (see text) on (a) grain size d , for $h=d/4$ (curves *1* and *1'*), $h=d/2$ (curves *2* and *2'*) and $h=3d/4$ (curves *3* and *3'*); and (b) parameter h at d=50 nm (curves *1* and *1'*), d=75 nm (curves *2* and *2'*) and d=100 nm (curves *3* and *3'*). Solid and dashed curves correspond τ=0 and 200 MPa, respectively.

Shockley dislocations and the residual screw dislocation). In these circumstances, s_0 has been calculated as that corresponding to extremum of $E_2(s)$ (given by formula (6)) at certain values of d, h and τ. For illustration of the size effect on the stacking fault width, we have calculated ratio s_0/s^*, where s^* is the stacking fault width in an infinite medium, at various values of the grain size d and parameter h. The dependence of ratio s_0/s^* on d, for the shear stress values τ=0 and 200 MPa, $h=d/4$ (see curves *1* and *1'*), $h=d/2$ (see curves *2* and *2'*) and $h=3d/4$ (see curves *3* and *3'*) are presented in Fig. 5a. The dependences of s_0/s^* on h, for t =0 and 200 MPa, d=50 nm (see curves *1* and *1'*), d=75 nm (see curves *2* and *2'*) and d=100 nm (see curves *3* and *3'*) are presented in Fig. 5b. The solid and dashed curves in Fig. 5 correspond to τ=0 and 200 MPa, respectively. Notice that s^*=0.457 nm for Al characterized by the stacking fault energy density γ=0.122 J/m^2. As follows from Fig. 5, the value of s_0 in a nanocrystalline Al is by several (up to 10) times larger than the stacking fault width s^* in coarse-grained Al. This theoretical result is in agreement with experimental data [23].

Let us compare results of our model with those of the model [23]. To do so, ratio s_0/s_l as a function of d, where s_l is the stacking fault width calculated by Liao *et al* [23], is shown in Fig. 6. In this situation, for definiteness, h is taken as $d/2$. Curves *1*, *2* and *3* in Fig. 6 correspond to τ=0, 100 and 200

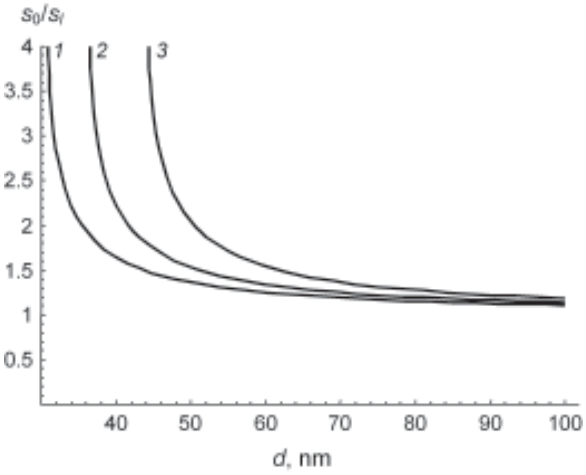

Fig. 6. Dependence of ratio s_0/s_l (see text) on grain size d, for $h=d/2$ and $\tau=0$, 100 and 200 MPa (curves *1*, *2* and *3*, respectively).

MPa, respectively. As follows from Fig. 6, our model gives larger values of the stacking fault width, compared to those given by the first approximation model [23]. In the physically interesting range of parameters, ratio s_0/s_l ranges from 1.5 to 2.

5. CONCLUDING REMARKS

Thus, in this paper a theoretical model has been elaborated describing partial and split dislocation configurations in deformed nanocrystalline metals. In the framework of the model (which modifies the first approximation model [23] by Liao *et al*), the energy characteristics of partial and split dislocations emitted from grain boundaries in nanocrystalline metals have been calculated. With these calculations, we found the ranges of parameters (grain size, applied stress, etc.) in which partial and split dislocation configurations are energetically favorable. Also, the width of stacking faults associated with split dislocations (Fig. 1b) has been shown to be larger than that in conventional coarse-grained polycrystals. The model accounts for the experimentally observed [23] formation of anomalously wide stacking faults bounded by partial dislocations in nanocrystalline Al.

ACKNOWLEDGEMENTS

The work was supported, in part, by INTAS (grant 03-51-3779), the Office of US Naval Research (grant N00014-01-1-1020), Russian Science Support Foundation, Russian Fund of Basic Research (grant 04-01-00211), Russian Academy of Sciences Program 'Structural Mechanics of Materials and Construction Elements', St.Petersburg Scientific Center, 'Integration' Program (grant B0026) and 'Dynasty' Foundation.

REFERENCES

[1] *Nanomaterials for Structural Applications*, MRS Symp Proc., Vol. 740, ed. by C.C. Berndt, T. Fischer, I.A. Ovid'ko, G. Skandan and T. Tsakalakos (MRS, Warrendale, 2003).
[2] *Mechanical Properties of Nanostructured Materials and Nanocomposites*, MRS Symp Proc., Vol. 791, ed. by I.A. Ovid'ko, C.S. Pande, R. Krishnamoorti, E. Lavernia and G. Skandan (MRS, Warrendale, 2004).
[3] F.A. Mohamed and Y. Li // *Mater. Sci. Eng. A* **298** (2001) 1.
[4] K.S. Kumar, S. Suresh, M.F. Chisholm, J.A. Horton and P. Wang // *Acta Mater.* **51 (**2003) 387.
[5] M.Yu. Gutkin and I.A. Ovid'ko, *Plastic Deformation in Nanocrystalline Materials* (Springer: Berlin, New York, *etc*., 2004).
[6] H. Hahn and K.A. Padmanabhan // *Phil. Mag. B* **76** (1997) 559.
[7] D.A. Konstantinidis and E.C. Aifantis // *Nanostruct. Mater.* **10** (1998) 1111.
[8] I.A. Ovid'ko // *Phil. Mag. Lett.* **83** (2003) 611.
[9] M.Yu. Gutkin, I.A. Ovid'ko and N.V. Skiba // *Acta Mater*. **52** (2004) 1711.
[10] M.Yu.Gutkin, I.A Ovid'ko and C.S.Pande // *Philos. Mag.* **84** (2004) 847.
[11] R.A. Masumura, P.M. Hazzledine and C.S. Pande // *Acta Mater*. **46** (1998) 4527.
[12] H.S. Kim, Y. Estrin and M.B. Bush // *Acta Mater.* **48** (2000) 493.
[13] V. Yamakov, D. Wolf, S.R. Phillpot and H. Gleiter // *Acta Mater.* **50** (2002) 61.
[14] M. Ke, S.A. Hackney, W.W. Milligan and E.C. Aifantis // *Nanostruct. Mater.* **5** (1995) 689.
[15] M. Murayama M, J.M. Howe, H. Hidaka and S. Takaki // *Science* **295** (2002) 2433.
[16] I.A. Ovid'ko // *Science* **295** (2002) 2386.
[17] M.Yu. Gutkin, I.A. Ovid'ko and N.V. Skiba // *Acta Mater.* **51** (2003) 4059.
[18] M.Yu. Gutkin and I.A. Ovid'ko // *Rev. Adv. Mater. Sci.* **4** (2003) 79.
[19] M. Chen, E. Ma, K.J. Hemker, H. Sheng, Y. Wang and X. Cheng // *Science* **300** (2003) 1275.

[20] X.Z. Liao, F. Zhou, E.J. Lavernia, S.G. Srinivasan, M.I. Baskes, D.W. He and Y.T. Zhu // *Appl. Phys. Lett.* **83** (2003) 632.
[21] X.Z. Liao, F. Zhou, E.J. Lavernia, D.W. He and Y.T. Zhu // *Appl. Phys. Lett.* **83** (2003) 5062.
[22] X.Z. Liao, Y.H. Zhao, S.G. Srinivasan, Y.T. Zhu, R.Z. Valiev and D.V. Gunderov // *Appl. Phys. Lett.* **84** (2004) 592.
[23] X.Z. Liao, S.G. Srinivasan, Y.H. Zhao, M.I. Baskes, Y.T. Zhu, F. Zhou, E.J. Lavernia and H.F. Xu // *Appl. Phys. Lett.* **84** (2004) 3564.
[24] S.V. Bobylev, M.Yu. Gutkin and I.A. Ovid'ko // *Acta Mater.* **52** (2004) 3793.
[25] J.P. Hirth and J. Lothe, *Theory of Dislocations* (McGraw-Hill: New York, 1982).